

Randomized Trial

Selection of the Optimal Puncture Needle for Induction of a Rat Intervertebral Disc Degeneration Model

Jiale Qian, MD^{1,2}, Jun Ge, MD¹, Qi Yan, MD¹, Cenhao Wu, MD¹, Huilin Yang, MD, PhD¹, and Jun Zou, MD, PhD¹

From: ¹Department of Orthopaedic Surgery, The First Affiliated Hospital of Soochow University, Suzhou, Jiangsu, China; ²Department of Orthopaedic Surgery, Suzhou Dushuhu Public Hospital, Suzhou, Jiangsu, China

Address Correspondence:
Jun Zou, MD, PhD
Department of Orthopaedic Surgery,
The First Affiliated Hospital of Soochow
University
188 Shizi St.
Suzhou, Jiangsu 215006, China
E-mail: jzou@suda.edu.cn

Disclaimer: Jiale Qian and Jun Ge contributed equally to this article. This study was supported by the National Natural Science Foundation of China (81472132, 81572183, 81672220, and 91849114), Priority Academic Program Development of Jiangsu Higher Education Institutions (PAPD).
Conflict of interest: Each author certifies that he or she, or a member of his or her immediate family, has no commercial association (i.e., consultancies, stock ownership, equity interest, patent/licensing arrangements, etc.) that might pose a conflict of interest in connection with the submitted manuscript.

Manuscript received: 11-03-2018
Revised manuscript received:
02-08-2019
Accepted for publication:
02-14-2019

Free full manuscript:
www.painphysicianjournal.com

Background: The incidence of intervertebral disc (IVD) degeneration has increased in recent years. A simple, reliable, and reproducible animal model is critical for understanding the underlying mechanisms of IVD degeneration. The caudal discs of rats have been proposed as a common puncture model in which to induce IVD degeneration. However, there is still no consensus on the size of needle to be used.

Objectives: The present study aimed to identify the appropriate needle size to establish an IVD degeneration model.

Study Design: A randomized, experimental trial.

Setting: Department of Orthopaedic Surgery, The First Affiliated Hospital of Soochow University, China.

Methods: Validity was verified by magnetic resonance imaging (MRI) and histology.

Results: From T2-weighted MRI imaging and histological examination, the IVD punctured by the 16-gauge needle degenerated acutely one week after the operation, whereas the 26-gauge needle puncture did no harm to the IVD. An 18-gauge needle showed a progressive degeneration in IVD.

Limitations: The observation period was not very long (4 weeks).

Conclusions: An 18-gauge needle can be used to induce IVD degeneration in rats. Therefore, an 18-gauge needle is the optimal selection to establish the degenerative IVD model on rats, whereas the 26-gauge needle failed to cause IVD degeneration. Thus, to study the prevention and treatment of IVD degeneration, a 26-gauge needle can be used for IVD injection of growth factors, plasmids, and drugs. A 16-gauge needle may be used to induce acute disc injury, but not IVD degeneration.

Key words: Low back pain, degenerative intervertebral disc, animal model, puncture needle, rat model, optimal choice

Pain Physician 2019; 22:353-360

In recent years, low back pain caused by intervertebral disc (IVD) degeneration has become a common disease. Epidemiologic surveys indicate that IVD disorders occur in about 90% of individuals aged > 60 years, seriously affecting their quality of life. Therefore, elucidating the pathogenesis of IVD disorders, as well

as identifying preventative measures and treatment options are critical research points that require animal models for investigation.

Several methods can be used to induce IVD degeneration. The biomechanical property of the IVD can be changed using a mechanical stress model (1,2) or spinal

instability model (3,4). Annulus fibrosus (AF) incision (5), endplate injury (6), and retroperitoneal drilling (7) can be conducted to disrupt the AF and endplate cartilage. The nucleus pulposus (NP) can be destroyed via injection of chemicals that dissolve the NP (8) or NP aspiration. Furthermore, IVD degeneration can be induced via gene knock-out, such as by induction of HLA-B27 expression (9) or type II collagen degeneration (10). Additionally, Yuan et al (11) recently evaluated the causal relationship between IVD degeneration and the blocking of the main blood supply gateway through the endplate. They established an IVD degeneration model by inducing an ischemic sub-endplate in the rat tail. It is critical to establish an ideal animal model to elucidate the pathogenesis of IVD degeneration (12).

In recent years, a novel IVD degeneration model, namely the puncture model caudal discs of rat tail, has been put forward and gradually accepted by more and more scholars (13). However, there is still no consensus on the size of the needle to be used during this procedure. The present study aimed to determine the optimal size of the needle that is required to establish a rat model of IVD degeneration. This model was verified by magnetic resonance imaging (MRI) and histology, thus providing a reliable animal model of IVD degeneration.

METHODS

Animals

A total of 24 male Sprague Dawley (SD) rats (aged 3 months, weighing 400 ± 20 g) were provided from the animal center of Soochow University. MRI and x-ray were used to exclude congenital malformation of the caudal vertebra and degenerative disc disease. Animals were randomly divided into 4 groups: 1 control group and 3 experimental groups. All groups included 6 rats. Each rat was individually housed in a dedicated room under a controlled temperature of 25°C.

Model Establishment

The experimental procedure was approved by the animal committee of The First Affiliated Hospital of Soochow University. Before the operation, x-ray was used to locate the IVDs, including coccygeal 7/8 (Co7/8), coccygeal 8/9 (Co8/9), and coccygeal 9/10 (Co9/10). Rats were weighed and anesthetized with 10% chloral hydrate (3.5 mL/kg) via peritoneal injection. After successful anesthetization, the percutaneous needle puncture technique was performed with 16-, 18- or 26-gauge needles at Co7/8, Co8/9, and Co9/10, respectively. The

needle perpendicularly punctured the rat tail, penetrated the contralateral skin, was rotated 360°, and held for 30 seconds. After operation, rats were provided free access to food and water and were monitored for postoperative complications such as uroschisis and infection. To evaluate the degree of disc degeneration, one of the experimental groups was randomly selected 1, 2, and 4 weeks postoperatively. Rats from the negative control group were euthanized for the further histological evaluation.

During needle puncture, the following points should be considered. First, to avoid damaging the upper and lower endplates and the periosteum of the vertebral body, and to prevent osteophyte formation and IVD segment stability subsequently, the needle point should enter at the center of the IVD (14). Additionally, the IVD segment needle puncture time should be the exact same to produce a consistent degree of IVD degeneration (15). Finally, the puncture direction should be vertical to the longitudinal axis of the IVD.

MRI Examination

Rats were anesthetized with 10% chloral hydrate (3.5 mL/kg) via peritoneal injection. After anesthetization, IVD signals in the experimental groups were obtained on a 1.5T MRI scanner (Philips Medical Systems, Andover, Massachusetts, USA), using the following parameters of T2-weighted sagittal plane: repetition time/echo time: 3500/102 ms, field of view: 15.0, thickness: 3 mm, interval: 0 mm. The degree of disc degeneration was assessed by signal intensity on T2-weighted imaging (T2WI) of IVD, and graded with a 4-grade modified Thompson system: grade 1: normal; grade 2: slightly decreased signals and obvious reduced high-signal areas; grade 3: moderately decreased signals; and grade 4: significantly reduced signals.

Histological Examination

After MRI, animals were euthanized and IVDs (Co7-8, Co8-9, and Co9-10) were harvested, fixed in 10% neutral formalin for 24 hours, and decalcified in 10% ethylenedinitrilo tetraacetic acid (EDTA) for 2 weeks. The IVD was cut into 4- μ m slices for hematoxylin and eosin (HE) staining. Slices were dewaxed in xylene twice for 5 minutes, dehydrated in graded ethanol (100%, 2 minutes; 95%, 1 minute; 80%, 1 minute; 75%, 1 minute), and stained with hematoxylin for 5 minutes and eosin for 2 minutes. The morphology of the IVD was scored under a light microscope according to Table 1. The method of euthanasia conforms to the animal

ethics and was approved by the animal committee.

Immunohistochemical Staining of Type II Collagen

The expression of type II collagen was detected using immunohistochemistry. In brief, slices were dewaxed in xylene, dehydrated in graded ethanol, incubated in 3% H₂O₂ at 37°C for 10 minutes, washed in phosphate-buffered saline solution for 5 minutes 3 times, boiled in 0.01 M citric acid buffer for antigen retrieval (95°C, 15-20 minutes), and blocked in goat serum for 10 minutes at 37°C. Slices were then incubated with primary antibody at 4°C overnight, and biotin labelled secondary antibody for 30 minutes at 37°C. Slices were counterstained with HE and observed under a light microscope at 400x magnification.

Statistical Analysis

The nonparametric Kruskal-Wallis and the Mann-Whitney U tests of MRI observations and histological grade were performed using SPSS 17.0 software (SPSS Inc., Chicago, IL). A $P < 0.05$ was regarded as statistically significant.

RESULTS

MRI

One week after surgery, disc Co7/8, punctured with a 16-gauge needle, presented decreased signals with reduced high-signal areas. Discs Co8/9 and Co9/10, punctured with 18- and 26-gauge needles, respectively, exhibited high signals that were not different from that seen in the normal disc (Fig. 1A). Two weeks postoperatively, the signal from IVD Co7/8 further decreased and exhibited "dark disc" with diminished intervertebral space. Co8/9 signals began to decrease, whereas the Co9/10 signal remained unchanged (Fig. 1B). At 4 weeks from the initial injury, the MRI signal of Co8/9 decreased

Table 1. Grading for morphology.

| | | Morphology Change Under Optical Microscope | Grade |
|-----|----------------------------|---|-------|
| I | Annulus Fibrosus (AF) | Normal texture and free of damage and distortion | 1 |
| | | The damaged and distortion area is less than 30% | 2 |
| | | The damaged and distortion area is more than 30% | 3 |
| II | Boundary between AF and NP | Normal | 1 |
| | | Micro disrupted | 2 |
| | | Medium or severe disrupted | 3 |
| III | NP Cells | Normal cells with large amounts of vacuoles | 1 |
| | | Cells and vacuoles decreased slightly | 2 |
| | | Cells decreased moderately or severely without vacuoles | 3 |
| IV | NP Matrix | Normal gel appearance | 1 |
| | | Slightly congealed | 2 |
| | | Moderate or severe condensation | 3 |

further, whereas the Co9/10 signal remained unchanged (Fig. 1C). One week postoperatively, the Thompson scores of Co7/8 were significantly higher than the normal disc (normal disc Thompson Score = 1; $P < 0.05$). Four weeks after needle puncture, the Thompson scores of the 18-gauge needle-punctured disc were significantly increased compared with the first week. Four weeks postoperatively, Co9/10 signal was slightly increased and presented no statistic differences when compared to the normal disc ($P > 0.05$, Fig. 2).

Histology

One week after puncture, the NP of disc Co7/8 was shrunken or absent, with a disordered or damaged AF. Moreover, an indistinct boundary was noticed between the AF and the NP. The size of the NP was reduced with time and had even been replaced by fibrous tissue (Fig. 3A, D, and G). One week after surgery, the NP of disc Co8/9 displayed a rounded shape and had a distinct border separating it from the surrounding AF. We also observed rounded and dispersive cells and an intact AF. Two weeks later, the NP began to shrink, and the AF was twisted. Four weeks later, the NP was even smaller, and the AF was disordered (Fig. 3B, E, and H). The NP of IVD Co9/10 only decreased 4 weeks after surgery and had a slightly ruptured AF (Fig. 3C, F, and I). According to the histological scoring system, the one-week postoperative evaluation showed that Co7/8 scores significantly increased in a time-dependent manner ($P < 0.05$), and the scores of Co8/9 were significantly different 4 weeks after surgery. No significant differences in score were observed in Co9/10 ($P > 0.05$, Fig. 4).

Immunohistochemical Staining of Type II Collagen

One week after surgery, the expression of type II collagen in IVD Co7/8 decreased in a time-dependent manner (Fig. 5A, D, and G). Two weeks later, type II collagen levels in Co8/9 began to decrease (Fig. 5B, E, and H). The expression of type II collagen in Co9/10 showed no changes compared to the normal disc, and the NP was yellow or

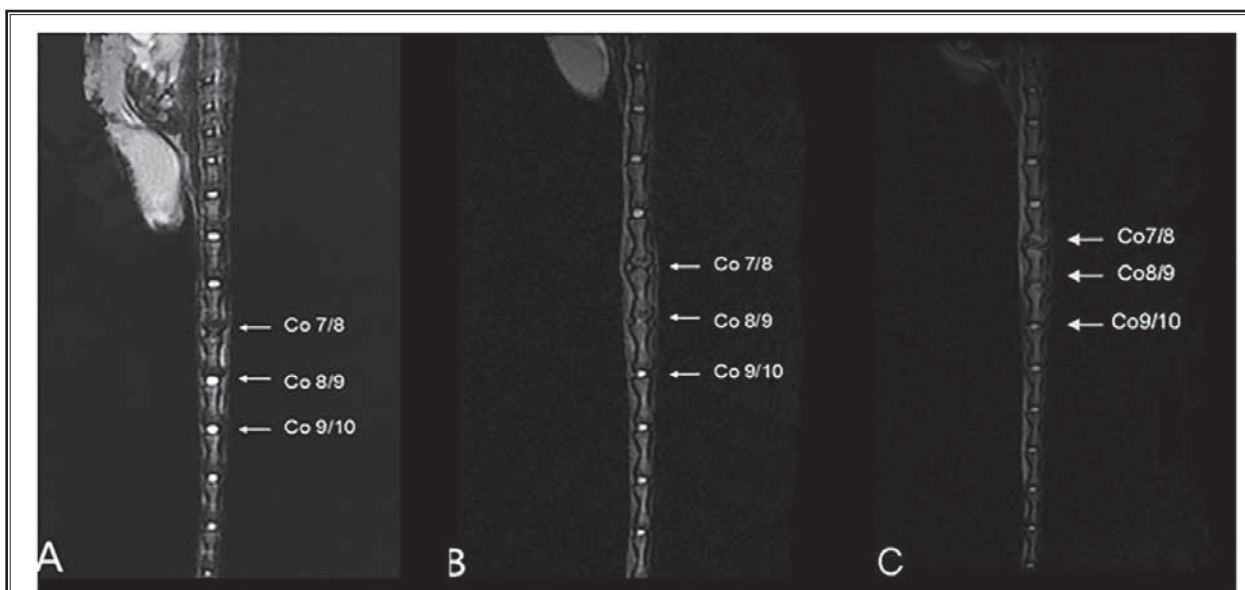


Fig. 1. *A) One week after operation, Co 7/8 (16G) presented decreased signals. Co8/9 (18G) and Co9/10 (26G) exhibited high signals like normal disc. B) Two weeks after operation, the signal from intervertebral disc Co7/8 (16G) further decreased. Co8/9(18G) signals began to decrease. Co9/10 (26G) signal remained unchanged. C) Four weeks later, the MRI signal of Co8/9(18G) decreased further, while the Co9/10 (26G) signal remained unchanged.*

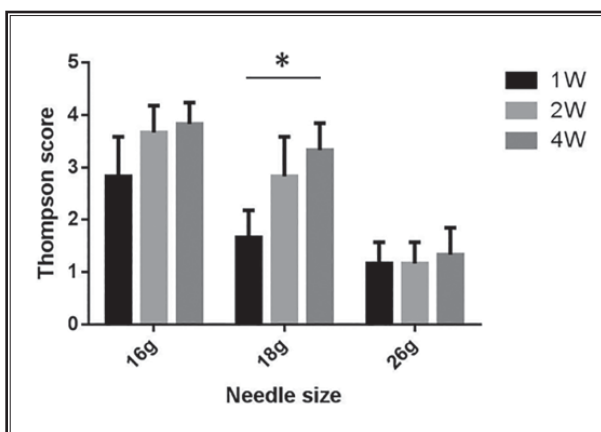
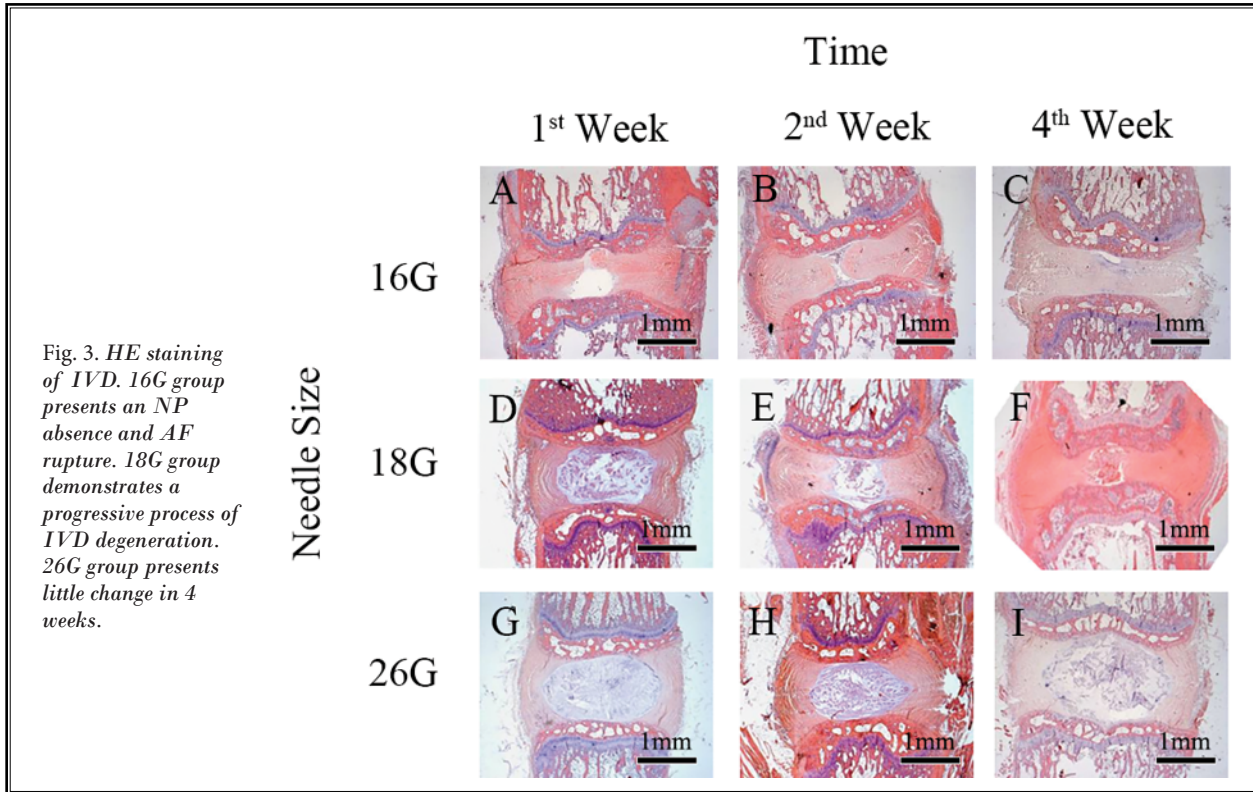


Fig. 2. *Thompson scores of 16G group were significantly higher than 1. Thompson scores of the 18G group at 4th week were significantly increased compared to the first week ($P < 0.05$). 26G group present slightly increasing in 4 weeks ($P > 0.05$).*

yellowish-brown (Fig. 5C, F, and I). These results indicate that puncture with a 16- or 18-gauge needle, and not a 26-gauge needle, lead to the reduced expression of type II collagen within the IVD.

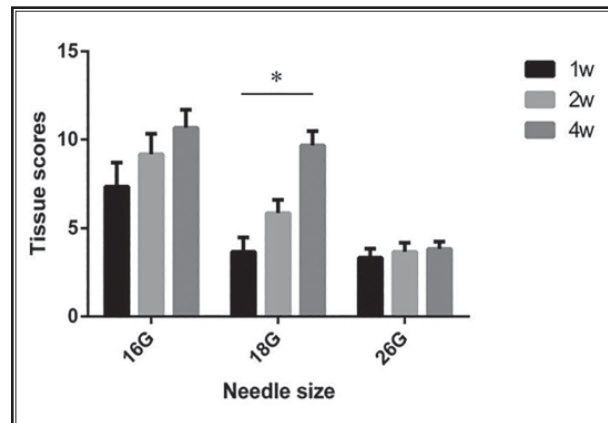
DISCUSSION

Animal models of IVD degeneration differ in their reliability and reproducibility (16). Because of their similarity to humans in both anatomic structure and physiological features, primates are the optimal IVD degeneration model. However, due to ethical limitations and high costs, large-scale studies using primates are limited. The use of mammals, including pigs and dogs, in large-scale investigations are also limited because of their high cost, difficulty in model establishment, high-standard experimental conditions, long experimental cycle, and poor reproducibility. In addition, the use of rabbits, frequently used in laboratory experiments, are limited owing to the complexity of model establishment, high infection rate, and lack of availability of relevant antibodies for the further research, whereas rats are better than the animals mentioned earlier on account of the cost and availability of relevant antibodies. Compared with the lumbar IVD, caudal IVD of rats is even easier to be located and operated. Several studies have carried out the research based on the rat caudal discs, especially in morphologic, biologic, and molecular research (17-20). As a novel animal model, it has been accepted by more and more scholars. We believed the caudal IVD of SD rats were beneficial to be used in this

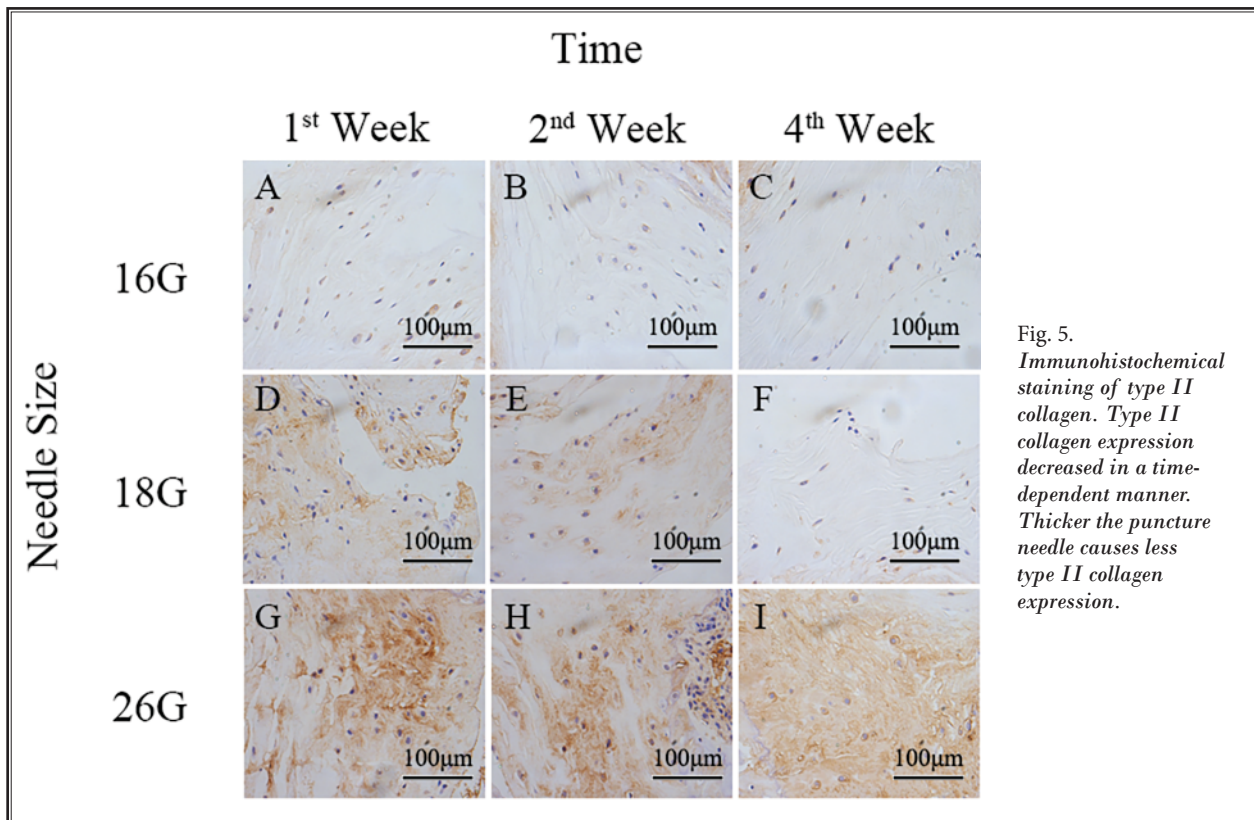


study because of their similarity to human biochemical components (16,21,22), ease of use in simple and reproducible procedures, and availability of relevant antibodies.

In this study, the AF was disrupted to induce IVD degeneration. This method, first applied on dogs by Key and Ford (23) in 1948, is commonly used in the laboratory testing. The mechanism of AF injury is not fully elucidated. Some scholars suggest that rupture of the AF activates an immune response and apoptosis in NP cells, resulting in the degeneration of the IVD (24,25). In addition, blood to the outer AF is supplied by the micro vessels in the spinal artery, whereas the inner AF and the NP have no blood supply, obtaining their nutrition from the cartilage endplates. Based on their theory, Eyre et al (26) showed that the outer AF was more capable of repair than the inner AF. Such properties make AF repair a key determinant for IVD degeneration. Lotz et al (27) suggested that the damaged AF is an open structure, and that the volumetric pressure of the NP is unbalanced, resulting in acute disc protrusion, decreased NP pressure, and finally disc degeneration. Although according to Hsieh et al (28), degenerative annular changes induced by puncture are



associated with inadequate biomechanical functioning of the disc. Generally speaking, a relatively large discontinuity of AF would be highly possible to cause the IVD degeneration, including fibrous replacement of the



nucleus, loss of type II collagen, aggrecan and water, and osteophyte formation, and others (27,29).

As T2WI signal intensity sensitively reflects changes in water, hydrogen, and proteoglycan content, MRI is the most direct and objective method to evaluate disc degeneration (30). Degenerative discs are characterized by decreased T2WI high-signal intensity and area. Additionally, HE staining is an important method used to observe tissue morphology. As the AF and NP are clearly detected under a microscope, it is easy to evaluate the degree of disc degeneration. The normal AF consists of several layers of fibrocartilage made up of fibroblast-like cells (outer layer) and chondrocyte-like cells (inner layer), whereas the NP is mainly composed of notochordal cells and chondrocyte-like cells. Degenerative discs present with disordered AF layers, increased cell death, a shrunken NP, and fibrochondrocyte-like tissue. In addition, degeneration of the IVD leads to the death of notochord cells and chondrocyte-like cells, osteophyte formation in the cartilage, and an indistinct boundary between the AF and NP (31). Immunohistochemistry is efficient for evaluating the degree of disc degeneration. Type II collagen is the main component

of the NP, and its content is decreased in degenerative IVD. Thus, the expression of type II collagen is an indicator used to evaluate the degree of disc degeneration.

According to Hsieh et al (28), annular defects should be large enough to prolong the duration of impaired disc function instead of being sealed and healed. Elliott et al (32) has revealed that the ratio of the needle diameter to the height of the punctured disc should be over 40% to induce significant IVD degeneration. Some research used a surgical blade, which is relative larger than the 40% of disc height, to establish IVD degeneration on rat (5), rabbit (14,33), dog (34), pig (35), and others. Both histology and radiology degeneration were achieved. However, on account of the large incision, it seems that stabbing was less controllable than needle puncture for inducing disc degeneration (14). Kim et al (36) compared the differences between puncture with a 21-gauge needle 3 times and an 18-gauge needle one time, and found that the former contained less water, as shown by MRI examination. Moreover, both showed significant reductions in IVD signal compared to the normal disc. Their study confirmed that both the 18- and 21-gauge needles were capable of inducing

IVD degeneration in rats. Sobajima et al (15) punctured the rat AF to a depth of 5 mm with a 16-gauge needle. MRI showed a reduction in the signal intensity of IVD 3 weeks postoperatively. Meanwhile, x-ray examination indicated osteophyte formation, and histological staining revealed reduced notochordal cells replaced by fibrous cartilage in the NP. These studies suggest that the degeneration of IVD is determined by the degree of injury in the AF and that excessive disc defects cause acute protrusion and acute degeneration of the NP. Thus, it is critical to create an optimal sized disc defect that induces disc degeneration without protrusion of the NP.

In our study, 3 gauges of needles were used for disc puncture. MRI, histological, and immunohistochemical analysis showed that puncture with a 16-gauge needle induced IVD degeneration one week after operation, and fibrosis also occurred 2 weeks postoperatively. This may result from the large needle size and acute IVD injury. Puncture with a 26-gauge needle did not

induce significant IVD degeneration. Puncture with an 18-gauge needle caused disc degeneration 2 weeks after operation, mimicking chronic IVD degeneration. Our results, obtained using the SD rat model of IVD degeneration, were consistent with that of previous studies. Based on our study, the 18-gauge needle was optimal for disc puncture and the 26-gauge needle could not induce disc degeneration. Thus, the 26-gauge needle may be used for injection of growth factors, plasmids, or drugs to study the prevention and treatment of IVD degeneration.

CONCLUSIONS

To establish a degenerative IVD rat model, an 18-gauge needle is the optimal choice, although a 26-gauge needle can be used to inject growth factors, plasmids, or drugs to study the prevention and treatment of IVD degeneration. A 16-gauge needle may be used to induce acute disc injury, but not IVD degeneration.

REFERENCES

1. Yamada K. The dynamics of experimental posture. Experimental study of intervertebral disk herniation in bipedal animals. *Clin Orthop* 1962; 25:20-31.
2. Cassidy JD, Yong-Hing K, Kirkaldy-Willis WH, Wilkinson AA. A study of the effects of bipedism and upright posture on the lumbosacral spine and paravertebral muscles of the Wistar rat. *Spine* 1988; 13:301-308.
3. Stokes IA, Counts DF, Frymoyer JW. Experimental instability in the rabbit lumbar spine. *Spine* 1989; 14:68-72.
4. Miyamoto S, Yonenobu K, Ono K. Experimental cervical spondylosis in the mouse. *Spine* 1991; 16:S495-500.
5. Rousseau MA, Ulrich JA, Bass EC, Rodriguez AG, Liu JJ, Lotz JC. Stab incision for inducing intervertebral disc degeneration in the rat. *Spine* 2007; 32:17-24.
6. Cinotti G, Della Rocca C, Romeo S, Vitur F, Toffanin R, Trasimeni G. Degenerative changes of porcine intervertebral disc induced by vertebral endplate injuries. *Spine* 2005; 30:174-180.
7. Lim KZ, Daly CD, Ghosh P, Jenkin G, Oehme D, Cooper-White J, Naidoo T, Goldschlager T. Ovine lumbar intervertebral disc degeneration model utilizing a lateral retroperitoneal drill bit injury. *J Vis Exp* 2017:123.
8. Kiester DP, Williams JM, Andersson GB, Thonar EJ, McNeill TW. The dose-related effect of intradiscal chymopapain on rabbit intervertebral discs. *Spine* 1994; 19:747-751.
9. Hammer RE, Maika SD, Richardson JA, Tang JP, Taurog JD. Spontaneous inflammatory disease in transgenic rats expressing HLA-B27 and human beta 2m: An animal model of HLA-B27-associated human disorders. *Cell* 1990; 63:1099-1112.
10. Sahlman J, Inkinen R, Hirvonen T, Lammi MJ, Lammi PE, Nieminen J, Lapveteläinen T, Prockop DJ, Arita M, Li SW, Hyttinen MM, Helminen HJ, Puustjärvi K. Premature vertebral endplate ossification and mild disc degeneration in mice after inactivation of one allele belonging to the Col2a1 gene for type II collagen. *Spine* 2001; 26:2558-2565.
11. Yuan W, Che W, Jiang YQ, Yuan FL, Wang HR, Zheng GL, Li XL, Dong J. Establishment of intervertebral disc degeneration model induced by ischemic sub-endplate in rat tail. *Spine J* 2015; 15:1050-1059.
12. Chen WH, Liu HY, Lo WC, Wu SC, Chi CH, Chang HY, Hsiao SH, Wu CH, Chiu WT, Chen BJ, Deng WP. Intervertebral disc regeneration in an ex vivo culture system using mesenchymal stem cells and platelet-rich plasma. *Biomaterials* 2009; 30:5523-5533.
13. Han B, Zhu K, Li FC, Xiao YX, Feng J, Shi ZL, Lin M, Wang J, Chen QX. A simple disc degeneration model induced by percutaneous needle puncture in the rat tail. *Spine* 2008; 33:1925-1934.
14. Masuda K, Aota Y, Muehleman C, Imai Y, Okuma M, Thonar EJ, Andersson GB, An HS. A novel rabbit model of mild, reproducible disc degeneration by an annulus needle puncture: Correlation between the degree of disc injury and radiological and histological appearances of disc degeneration. *Spine* 2005; 30:5-14.
15. Sobajima S, Kompel JF, Kim JS, Wallach CJ, Robertson DD, Vogt MT, Kang JD, Gilbertson LG. A slowly progressive and reproducible animal model of intervertebral disc degeneration characterized by MRI, x-ray, and histology. *Spine* 2005; 30:15-24.
16. O'Connell GD, Vresilovic EJ, Elliott DM. Comparison of animals used in disc re-

- search to human lumbar disc geometry. *Spine* 2007; 32:328-333.
17. Wu X, Liu Y, Guo X, Zhou W, Wang L, Shi J, Tao Y, Zhu M, Geng D, Yang H, Mao H. Prolactin inhibits the progression of intervertebral disc degeneration through inactivation of the NF-kappaB pathway in rats. *Cell Death Dis* 2018; 9:98.
 18. Ji ML, Jiang H, Zhang XJ, Shi PL, Li C, Wu H, Wu XT, Wang YT, Wang C, Lu J. Preclinical development of a microRNA-based therapy for intervertebral disc degeneration. *Nat Commun* 2018; 9:5051.
 19. Grunert P, Borde BH, Hudson KD, Macielak MR, Bonassar LJ, Härtl R. Annular repair using high-density collagen gel: A rat-tail in vivo model. *Spine* 2014; 39:198-206.
 20. Borde B, Grunert P, Hartl R, Bonassar LJ. Injectable, high-density collagen gels for annulus fibrosus repair: An in vitro rat tail model. *J Biomed Mater Res A* 2015; 103:2571-2581.
 21. Keorochana G, Johnson JS, Taghavi CE, Liao JC, Lee KB, Yoo JH, Ngo SS, Wang JC. The effect of needle size inducing degeneration in the rat caudal disc: Evaluation using radiograph, magnetic resonance imaging, histology, and immunohistochemistry. *Spine J* 2010; 10:1014-1023.
 22. de Campos MF, de Oliveira CP, Neff CB, Correa OM, Pinhal MA, Rodrigues LM. Studies of molecular changes in intervertebral disc degeneration in animal model. *Acta Orthop Bras* 2016; 24:16-21.
 23. Key JA, Ford LT. Experimental intervertebral-disc lesions. *J Bone Joint Surg Am* 1948; 30A:621-630.
 24. Olmarker K, Blomquist J, Stromberg J, Nannmark U, Thomsen P, Rydevik B. Inflammotogenic properties of nucleus pulposus. *Spine* 1995; 20:665-669.
 25. Satoh K, Konno S, Nishiyama K, Olmarker K, Kikuchi S. Presence and distribution of antigen-antibody complexes in the herniated nucleus pulposus. *Spine* 1999; 24:1980-1984.
 26. Eyre DR, Matsui Y, Wu JJ. Collagen polymorphisms of the intervertebral disc. *Biochem Soc Trans* 2002; 30:844-848.
 27. Lotz JC. Animal models of intervertebral disc degeneration: Lessons learned. *Spine* 2004; 29:2742-2750.
 28. Hsieh AH, Hwang D, Ryan DA, Freeman AK, Kim H. Degenerative anular changes induced by puncture are associated with insufficiency of disc biomechanical function. *Spine* 2009; 34:998-1005.
 29. Lipson SJ, Muir H. 1980 Volvo award in basic science. Proteoglycans in experimental intervertebral disc degeneration. *Spine* 1981; 6:194-210.
 30. Videman T, Nurminen M, Troup JD. 1990 Volvo Award in clinical sciences. Lumbar spinal pathology in cadaveric material in relation to history of back pain, occupation, and physical loading. *Spine* 1990; 15:728-740.
 31. Thompson JP, Pearce RH, Schechter MT, Adams ME, Tsang IK, Bishop PB. Preliminary evaluation of a scheme for grading the gross morphology of the human intervertebral disc. *Spine* 1990; 15:411-415.
 32. Elliott DM, Yerramalli CS, Beckstein JC, Boxberger JJ, Johannessen W, Vresilovic EJ. The effect of relative needle diameter in puncture and sham injection animal models of degeneration. *Spine* 2008; 33:588-596.
 33. Takaishi H, Nemoto O, Shiota M, Kikuchi T, Yamada H, Yamagishi M, Yabe Y. Type-II collagen gene expression is transiently upregulated in experimentally induced degeneration of rabbit intervertebral disc. *J Orthop Res* 1997; 15:528-538.
 34. Hampton D, Laros G, McCarron R, Franks D. Healing potential of the annulus fibrosus. *Spine* 1989; 14:398-401.
 35. Kanerva A, Kommonen B, Gronblad M, Tolonen J, Habtemariam A, Virri J, Karaharju E. Inflammatory cells in experimental intervertebral disc injury. *Spine* 1997; 22:2711-2715.
 36. Kim KS, Yoon ST, Li J, Park JS, Hutton WC. Disc degeneration in the rabbit: A biochemical and radiological comparison between four disc injury models. *Spine* 2005; 30:33-37.